

Self-Diffusion in Liquid Copper, Silver, and Gold

Nikolay Dubinin ^{1,2}

¹ Institute of Metallurgy of the Ural Branch of the Russian Academy of Sciences, 101 Amundsen st., 620016 Ekaterinburg, Russia; ned67@mail.ru

² Department of Rare Metals and Nanomaterials, Ural Federal University, 19 Mira st., 620002 Ekaterinburg, Russia

Received: 18 October 2020; Accepted: 4 December 2020; Published: 7 December 2020



Abstract: The recently developed by us semi-analytical representation of the mean spherical approximation in conjunction with the linear trajectory approximation is applied to the quantitative study of self-diffusivities in liquid Cu, Ag and Au at different temperatures. The square-well model is employed for the description of the interatomic pair interactions in metals under study. It is found that our theoretical results are in good agreement with available experimental and computer-simulation data and can be considered as a prediction when such data are absent.

Keywords: liquid metal; diffusion; square-well model; mean spherical approximation; linear trajectory approximation

1. Introduction

An experimental study of diffusion properties in metal melts is a hard task. Progress in this field is connected with the arising of new techniques in the last two decades [1–20]. In particular, modern precise measurements provided a finding that small additions in dilute germanium weakly affect its diffusion coefficients in spite of the very big difference between their atomic mass [20]. Nevertheless, despite big progress spreading to binary and multicomponent alloys, the discrepancy in experimental results remains up to the present time, even for pure liquid metals. Therefore, theoretical approaches serve as an efficient instrument for investigations in this area. One of them is the square-well (SW) model, which is actively applied to liquid metals and their alloys [21–29].

In the last years, the square-well model and closely related to its models are intensively developed, including its applications to diffusivities' calculations [30–40]. Some years ago, we introduced the semi-analytical method [41] of solving the Ornstein–Zernike equation [42] for the SW model within the mean spherical approximation (MSA) [43]. Then, this method, in conjunction with the linear trajectory approximation (LTA) [44,45], was successfully used to calculate the self-diffusion coefficients of liquid alkali metals and their binary mixtures [46–48].

Here, we apply the aforementioned SW-MSA-LTA approach for the quantitative study of self-diffusivities in liquid noble metals and compare obtained results with available experimental and computer-simulation data.

2. Theory

In the majority of model theories, the Einstein relation is the basis for calculating the self-diffusion coefficient, D , of the atom in the pure liquid as a quantity which is inversely proportional to the friction coefficient, ξ , of the same atom [49]:

$$D = (\beta\xi)^{-1} \quad (1)$$

where $\beta = (k_B T)^{-1}$; k_B is the Boltzmann constant; T is the temperature.

In the theory of liquids, there are many ways to determine ξ [50,51]. Among them, the linear trajectory approximation is one of the best. It was introduced by Helfand [44] for fluids described by any hard-core (HC) pair potential, $\phi_{\text{HC}}(r)$, to take into account the non-hard-core contribution to the friction coefficient, $\xi_{\text{non-HC}}$:

$$\xi_{\text{non-HC}} = -\frac{(\beta\pi M)^{1/2}}{12\pi^2} \int_0^\infty [S(q) - 1] \varphi_{\text{HC}}(q) q^3 dq \quad (2)$$

Here, M is the atomic mass; $S(q)$ is the structure factor in the corresponding HC model; $\varphi_{\text{HC}}(q)$ is the Fourier transform of $\phi_{\text{HC}}(r)$ outside the hard core, $\varphi_{\text{HC}}(r)$:

$$\varphi_{\text{HC}}(q) = 4\pi \int_\sigma^\infty \phi_{\text{HC}}(r) \frac{\sin(qr)}{qr} r^2 dr \quad (3)$$

Together with the contribution from the hard-core part of the pair interaction, ξ_{HC} , suggested earlier in [52] the contribution $\xi_{\text{non-HC}}$ allows to write the total friction coefficient for pure liquids in the framework of the Helfand theory:

$$\xi = \xi_{\text{HC}} + \xi_{\text{non-HC}} \quad (4)$$

where

$$\xi_{\text{HC}} = \frac{8}{3} \rho \sigma^2 g(\sigma) (\pi M / \beta)^{1/2} \quad (5)$$

ρ is the mean atomic density, σ is the diameter of the hard core, $g(r)$ is the pair correlation function of the HC model under consideration.

Davis and Palyvos [45] modified Equation (4) by taking into account the cross effect between HC and non-HC forces:

$$\xi = \xi_{\text{HC}} + \xi_{\text{non-HC}} + \xi_{\text{cross}} \quad (6)$$

where

$$\xi_{\text{cross}} = -\frac{1}{3} \rho (\beta M / \pi)^{1/2} g(\sigma) \int_0^\infty [x \cos(x) - \sin(x)] \varphi_{\text{HC}}(q) dq, \quad (7)$$

$$x = q\sigma$$

As a hard-core potential, we take the square-well one:

$$\phi_{\text{SW}}(r) = \begin{cases} \infty, & r < \sigma \\ \varepsilon, & \sigma \leq r < \lambda\sigma \\ 0, & r \geq \lambda\sigma \end{cases} \quad (8)$$

where ε and $\sigma(\lambda - 1)$ are the depth and the width of the square well, respectively.

The Fourier transform (3) of its non-hard-core part leads to:

$$\phi_{\text{SW}}(q) = 4\pi\varepsilon [\sin(\lambda x) - \sin(x) - \lambda x \cos(\lambda x) + x \cos(x)] / q^3 \quad (9)$$

For the SW potential, Equations (2), (5) and (7) are being rewritten, respectively, as:

$$\xi_{\text{non-HC}} = -\frac{(\beta\pi M)^{1/2}}{12\pi^2} \int_0^\infty [S_{\text{SW}}(q) - 1] \phi_{\text{SW}}(q) q^3 dq \quad (10)$$

$$\xi_{\text{HC}} = \frac{8}{3} \rho \sigma^2 g_{\text{SW}}(\sigma) (\pi M / \beta)^{1/2} \quad (11)$$

$$\xi_{\text{cross}} = -\frac{1}{3}\rho (\beta M/\pi)^{1/2} g_{\text{SW}}(\sigma) \int_0^{\infty} [x \cos(x) - \sin(x)] \varphi_{\text{SW}}(q) dq \quad (12)$$

where

$$S_{\text{SW}}(q) = \frac{1}{1 - \rho c_{\text{SW}}(q)} \quad (13)$$

Here, $c_{\text{SW}}(q)$ is the Fourier transform of the SW partial direct correlation function, $c_{\text{SW}}(r)$. The calculation of $c_{\text{SW}}(q)$ is not a trivial task as it is for the analogous function within the hard-sphere model for which the analytical solution is known [53,54]. In our work, $c_{\text{SW}}(r)$ is represented in the semi-analytical form of the mean spherical approximation [41,47]:

$$c_{\text{SW}}(r) = \begin{cases} \sum_{m=0}^n b_m \left(\frac{r}{\sigma}\right)^m & r < \sigma \\ -\beta \varphi_{\text{SW}}(r), & r \geq \sigma \end{cases} \quad (14)$$

where $n \geq 3$; b_m are the coefficients determined during fulfilling the condition that the pair correlation function must be equal to zero inside the hard core:

$$g_{\text{SW}}(r) = 0 \text{ at } r < \sigma \quad (15)$$

The Fourier transform of Equation (14),

$$c(q) = 4\pi \int_0^{\infty} c(r) \frac{\sin(qr)}{qr} r^2 dr \quad (16)$$

gives

$$c_{\text{SW}}(q) = -\beta \varphi_{\text{SW}}(q) + \left(\frac{4\pi}{q^3}\right) \left\{ \sum_{m=1}^{n+2} x^{2-m} \frac{\partial^m \sin(x)}{\partial x^m} \sum_{l=0}^n b_l \prod_{k=0}^{m-2} (l+1-k) + \sum_{m=1}^{[(n+1)/2]} \frac{(-1)^{m+1} (2m)! b_{(2m-1)}}{x^{2m-1}} \right\} \quad (17)$$

where $[(n+1)/2]$ is the integral part of $(n+1)/2$.

To numerically solve Equation (15), we use the simplex method in conjunction with the Fourier transform of $g_{\text{SW}}(r)$,

$$g_{\text{SW}}(r) = 1 + \frac{1}{2\pi^2\rho} \int_0^{\infty} [S_{\text{SW}}(q) - 1] \frac{\sin(qr)}{qr} q^2 dq \quad (18)$$

at $n = 5$.

3. Results and Discussion

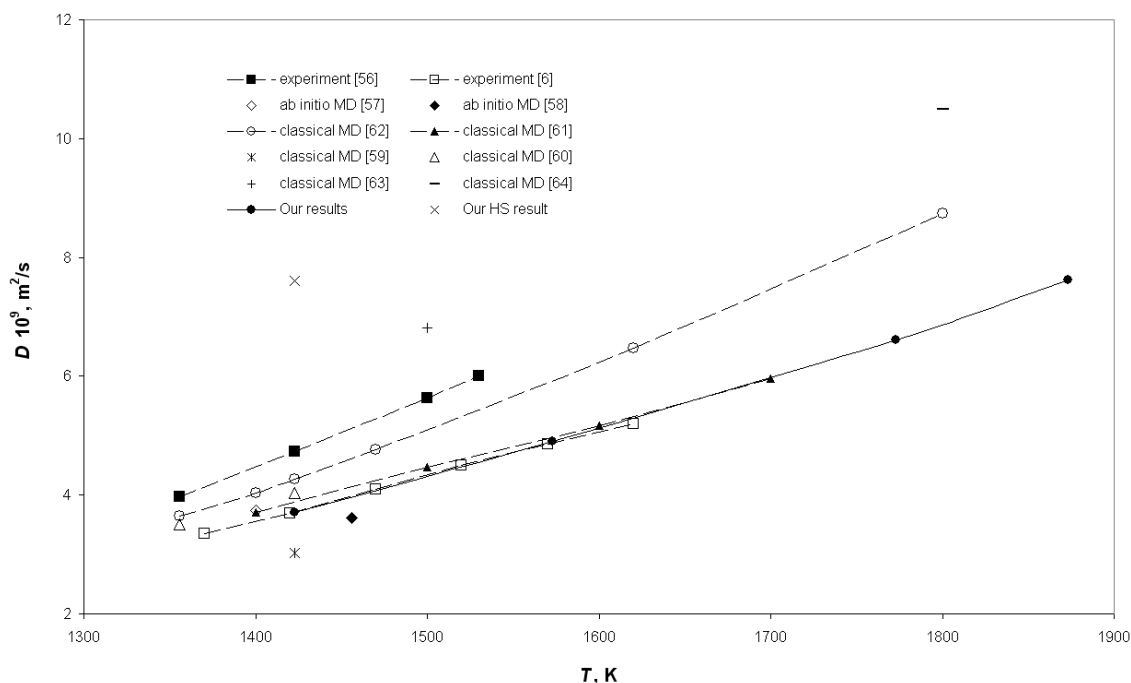
The calculations are fulfilled at temperatures at which the experimental information about the mean atomic densities and structure factors of liquid metals under consideration is available [55]. The corresponding values of T and ρ are listed in Table 1. Experimental $S(q)$ are needed to find adjustable values of the SW parameters by fitting the calculated structure factor with respect to the experimental one at each temperature.

Table 1. Input values of ρ (kg/m³) used for calculations.

Metal	$T = 1273$ K	$T = 1423$ K	$T = 1573$ K	$T = 1773$ K	$T = 1873$ K
Cu	-	7970	7860	7690	7620
Ag	9270	9120	8980	-	-
Au	-	17,200	17,100	16,900	-

The obtained results are represented in Figures 1–3, together with experimental, classical molecular dynamics (MD), and ab initio MD results available in the literature.

For liquid Cu (Figure 1), there are two experimental works on the self-diffusion coefficient [6,56]. Our results, as well as the ab initio MD [57,58] and classical MD [59–61] results, agree significantly better with the modern experiment of Meyer [6] rather than with one of Henderson and Yang [56] while the classical MD results of Mei and Davenport [62] are approximately equidistant from both experimental series. Note that other classical MD calculations [63,64] give essentially higher values of D even in comparison with the results of [56].

**Figure 1.** Self-diffusion coefficient of liquid Cu.

Our values of D for liquid Ag are lower than ones from all three experimental works [1,14,65]. However, the tendency to convergence with experimental data with an increase in the temperature is observed (Figure 2). A better agreement (deviation is less than 15%) is observed with more recent experimental results [14]. There is also good agreement with results [65] (which are extrapolated to different from available in the original work temperatures using the empirical relation from [51]). The accuracy of the experiment of Itami et al. [1] is not completely reliable to our opinion since the temperature dependence of the self-diffusion coefficient in [1] has the minimum at some temperature.

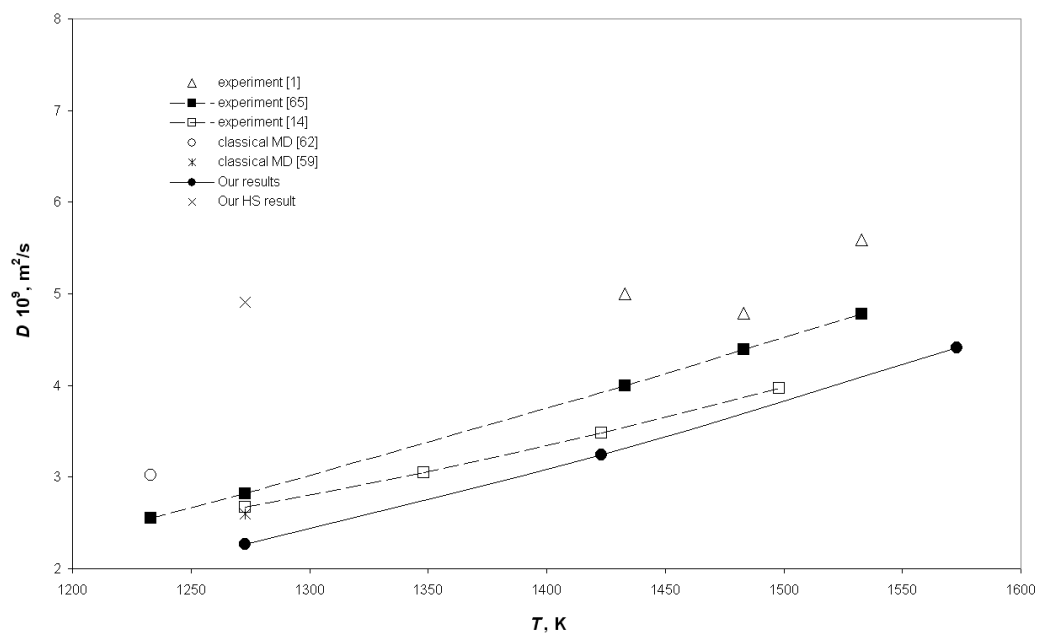


Figure 2. Self-diffusion coefficient of liquid Ag.

For liquid Au (Figure 3), the experimental results on the self-diffusion coefficient are not available. There are two ab initio [66,67] and three classical [59,62,68] MD simulations at different temperatures. The discrepancy between these results is very big. For example, the result of the work [62] obtained $T = 1336$ K is approximately three times bigger than the corresponding value of D which can be approximated from Figure 3 of the work [66] at the same temperature. On the whole, the classical MD simulations (except for [59]) give significantly higher values D than ab initio MD simulations. Our result lies very close to the ab initio MD results of Peng et al. [67], which are approximately average between the ab initio MD results of [66] and the classical MD result of [59].

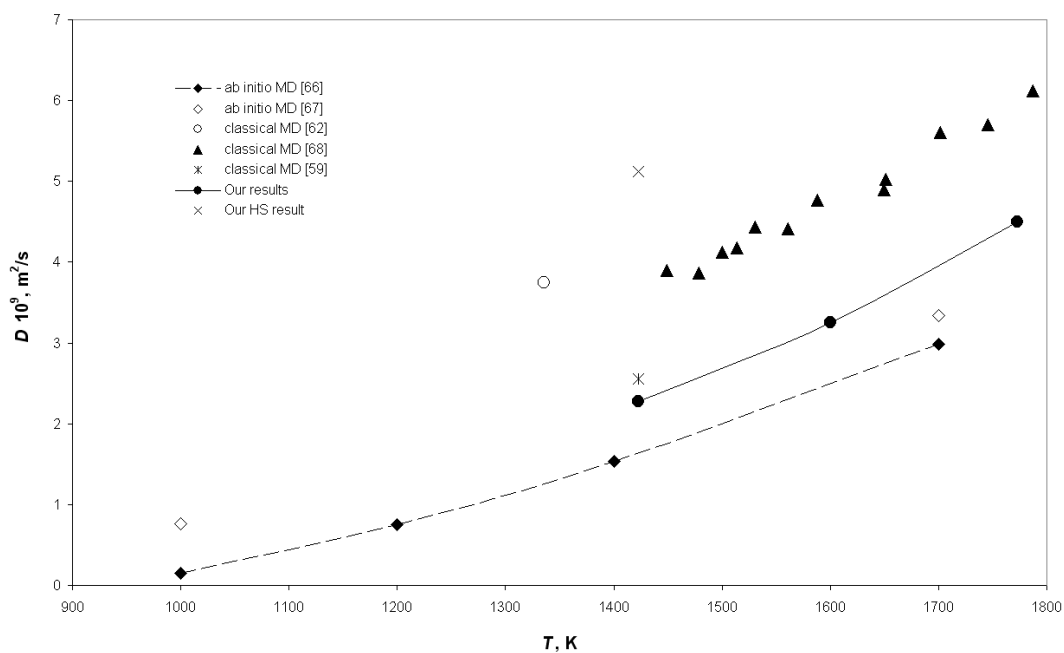


Figure 3. Self-diffusion coefficient of liquid Au.

Additionally, we calculated D within the hard-sphere (HS) model at the lowest among taken for each metal temperature (Figures 1–3). It is clear that the HS results are sufficiently crude.

4. Conclusions

In the present work, it is found that the semi-analytical representation of the mean spherical approximation applied to the square-well model in the frameworks of the linear trajectory approximation allows obtaining good quantitative results for the self-diffusivities in liquid noble metals. Moreover, as well as for alkali liquid metals and their alloys [46–48], this good description is achieved with the SW-parameters' values defined from the structure data that shows the universality of the used approach.

Funding: This work is supported by the Russian Federation Ministry of Science and Higher Education through the state research target for the Institute of Metallurgy of the Ural Branch of Russian Academy of Sciences (Project No. 0396-2019-0002).

Conflicts of Interest: The author declares no conflict of interest.

References

1. Itami, T.; Mizuno, A.; Aoki, H.; Arai, Y.; Goto, K.; Amano, S.; Tateiwa, N.; Kaneko, M.; Fukazawa, T.; Nakamura, R.; et al. The study of self-diffusion and mutual-diffusion of liquid Cu-Ag alloys. *J. Jpn. Soc. Microgravity Appl.* **2000**, *17*, 64–69.
2. Masaki, T.; Fukazawa, T.; Matsumoto, S.; Itami, T.; Yoda, S. Measurements of diffusion coefficients of metallic melt under microgravity—Current status of the development of shear cell technique towards JEM on ISS. *Meas. Sci. Technol.* **2005**, *16*, 327–335. [[CrossRef](#)]
3. Mathiak, G.; Plescher, E.; Willnecker, R. Liquid metal diffusion experiments in microgravity—Vibrational effects. *Meas. Sci. Technol.* **2005**, *16*, 336–344. [[CrossRef](#)]
4. Cahoon, J.R.; Jiao, Y.; Tandon, K.; Chaturvedi, M. Interdiffusion in liquid tin. *J. Phase Equilibria Diffus.* **2006**, *27*, 325–332. [[CrossRef](#)]
5. Meyer, A.; Stüber, S.; Holland-Moritz, D.; Heinen, O.; Unruh, T. Determination of self-diffusion coefficients by quasielastic neutron scattering measurements of levitated Ni droplets. *Phys. Rev. B* **2008**, *77*, 092201. [[CrossRef](#)]
6. Meyer, A. Self-diffusion in liquid copper as seen by quasielastic neutron scattering. *Phys. Rev. B* **2010**, *81*, 012102. [[CrossRef](#)]
7. Bartsch, A.; Rätzke, K.; Meyer, A.; Faupel, F. Dynamic Arrest in Multicomponent Glass-Forming Alloys. *Phys. Rev. Lett.* **2010**, *104*, 195901. [[CrossRef](#)]
8. Porth, C.B.; Cahoon, J.R. Interdiffusion of Bi in Liquid Sn. *J. Phase Equilibria Diffus.* **2010**, *31*, 149–156. [[CrossRef](#)]
9. Lee, N.; Cahoon, J.R. Interdiffusion of Copper and Iron in Liquid Aluminum. *J. Phase Equilibria Diffus.* **2011**, *32*, 226–234. [[CrossRef](#)]
10. Brillo, J.; Pommrich, A.I.; Meyer, A. Relation between Self-Diffusion and Viscosity in Dense Liquids: New Experimental Results from Electrostatic Levitation. *Phys. Rev. Lett.* **2011**, *107*, 165902. [[CrossRef](#)]
11. Weis, H.; Unruh, T.; Meyer, A. The measurement of self-diffusion coefficients in liquid germanium using quasielastic neutron scattering. *High Temp. High Press.* **2013**, *42*, 39–47.
12. Pommrich, A.I.; Unruh, T.; Meyer, A. Self-diffusion of 3d transition metals in liquid silicon alloys. *High Temp. High Press.* **2013**, *42*, 49–55.
13. Geng, Y.; Zhu, C.; Zhang, B. A sliding cell technique for diffusion measurements in liquid metals. *AIP Adv.* **2014**, *4*, 037102. [[CrossRef](#)]
14. Engelhardt, M.; Meyer, A.; Yang, F.; Simeoni, G.; Kargl, F. Self and Chemical Diffusion in Liquid Al-Ag. *Defect Diffus. Forum* **2016**, *367*, 157–166. [[CrossRef](#)]
15. Basuki, S.W.; Yang, F.; Gill, E.; Rätzke, K.; Meyer, A.; Faupel, F. Atomic dynamics in Zr-based glass forming alloys near the liquidus temperature. *Phys. Rev. B* **2017**, *95*, 024301. [[CrossRef](#)]
16. Zhong, L.; Hu, J.; Geng, Y.; Zhu, C.; Zhang, B. A multi-slice sliding cell technique for diffusion measurements in liquid metals. *Rev. Sci. Instruments* **2017**, *88*, 93905. [[CrossRef](#)]
17. Xiong, L.H.; Wang, X.D.; Cao, Q.P.; Zhang, D.X.; Xie, H.L.; Xiao, T.Q.; Jiang, J.Z. Composition- and temperature-dependent liquid structures in Al-Cu alloys: An ab initio molecular dynamics and X-ray diffraction study. *J. Phys. Condens. Matter* **2017**, *29*, 035101. [[CrossRef](#)]
18. Belova, I.; Heuskin, D.; Sondermann, E.; Ignatzi, B.; Kargl, F.; Murch, G.E.; Meyer, A. Combined interdiffusion and self-diffusion analysis in Al-Cu liquid diffusion couple. *Scr. Mater.* **2018**, *143*, 40–43. [[CrossRef](#)]

19. Sondermann, E.; Jakse, N.; Binder, K.; Mielke, A.; Heuskin, D.; Kargl, F.; Meyer, A. Concentration dependence of interdiffusion in aluminum-rich Al-Cu melts. *Phys. Rev. B* **2019**, *99*, 024204. [\[CrossRef\]](#)
20. Weis, H.; Kargl, F.; Kolbe, M.; Koza, M.M.; Unruh, T.; Meyer, A. Self- and interdiffusion in dilute liquid germanium-based alloys. *J. Phys. Condens. Matter* **2019**, *31*, 455101. [\[CrossRef\]](#)
21. Rao, R.V.G.; Bhattacharyya, M. Partial structures of compound-forming liquid gold–caesium alloy. A model potential approach. *Phys. Status Solidi* **1987**, *140*, 51–61. [\[CrossRef\]](#)
22. Venkatesh, R.; Rao, R. Total and partial structure factors, compressibility, diffusion coefficients and other associated properties of an Ag-Se semiconducting alloy. *J. Mol. Struct.* **1996**, *361*, 283–288. [\[CrossRef\]](#)
23. Anusionwu, B.C.; Akinlade, O.; Hussain, L.A. A Theoretical Study of Structure and Ordering in Pb-Bi Molten Alloys. *Phys. Chem. Liq.* **1997**, *34*, 1–13. [\[CrossRef\]](#)
24. Venkatesh, R.; Mishra, R.K.; Rao, R.V.G. Structural, thermodynamic and other associated properties of partially ordered Ag-In alloy. *Phys. Status Solidi* **2003**, *240*, 549–560. [\[CrossRef\]](#)
25. Grosdidier, B.; Gasser, J.-G. Ordering potential in liquid Al-Ge alloys structure and thermodynamics. *Intermetallics* **2003**, *11*, 1253–1258. [\[CrossRef\]](#)
26. Grosdidier, B.; Osman, S.M.; Ben Abdellah, A. Liquid gallium-lead mixture spinodal, binodal, and excess thermodynamic properties. *Phys. Rev. B* **2008**, *78*, 024205. [\[CrossRef\]](#)
27. Dubinin, N.; Filippov, V.; Malkhanova, O.; Vatolin, N. Structure factors of binary liquid metal alloys within the square-well model. *Cent. Eur. J. Phys.* **2009**, *7*, 584–590. [\[CrossRef\]](#)
28. Osman, S.M.; Grosdidier, B.; Ali, I.; Ben Abdellah, A. Liquid gallium-lead mixture phase diagram, surface tension near the critical mixing point, and prewetting transition. *Phys. Rev. E* **2013**, *87*, 062103. [\[CrossRef\]](#)
29. Dubinin, N.; Filippov, V.; Yuryev, A.; Vatolin, N. Excess entropy of mixing for binary square-well fluid in the mean spherical approximation: Application to liquid alkali-metal alloys. *J. Non-Cryst. Solids* **2014**, *401*, 101–104. [\[CrossRef\]](#)
30. Yu, Y.-X.; Han, M.-H.; Gao, G.-H. Self-diffusion in a fluid of square-well spheres. *Phys. Chem. Chem. Phys.* **2001**, *3*, 437–443. [\[CrossRef\]](#)
31. Krekelberg, W.P.; Mittal, J.; Ganesan, V.; Truskett, T.M. How short-range attractions impact the structural order, self-diffusivity, and viscosity of a fluid. *J. Chem. Phys.* **2007**, *127*, 044502. [\[CrossRef\]](#) [\[PubMed\]](#)
32. Srivastava, R.; Khanna, K. Self-diffusion coefficients of dense fluid for a square-well fluid. *J. Mol. Liq.* **2007**, *136*, 156–160. [\[CrossRef\]](#)
33. Ryltsev, R.E.; Chtchelkatchev, N.M.; Ryzhov, V.N. Superfragile Glassy Dynamics of a One-Component System with Isotropic Potential: Competition of Diffusion and Frustration. *Phys. Rev. Lett.* **2013**, *110*, 025701. [\[CrossRef\]](#) [\[PubMed\]](#)
34. Ryltsev, R.E.; Klumov, B.; Chtchelkatchev, N. Self-assembly of the decagonal quasicrystalline order in simple three-dimensional systems. *Soft Matter* **2015**, *11*, 6991–6998. [\[CrossRef\]](#) [\[PubMed\]](#)
35. Ryltsev, R.E.; Chtchelkatchev, N. Universal self-assembly of one-component three-dimensional dodecagonal quasicrystals. *Soft Matter* **2017**, *13*, 5076–5082. [\[CrossRef\]](#)
36. Torres-Carbajal, A.; Trejos, V.M.; Collazo, L.A.N. Self-diffusion coefficient of the square-well fluid from molecular dynamics simulations within the constant force approach. *J. Chem. Phys.* **2018**, *149*, 144501. [\[CrossRef\]](#)
37. Davydov, A.G.; Tkachev, N. Features of the dimerization equilibrium in square-well fluids. *J. Mol. Liq.* **2019**, *275*, 91–99. [\[CrossRef\]](#)
38. Fomin, Y. Anomalously high heat capacity of core-softened liquids. *Phys. Chem. Liq.* **2017**, *57*, 67–74. [\[CrossRef\]](#)
39. Tsiok, E.; Fomin, Y.D.; Ryzhov, V.N. The effect of confinement on the solid–liquid transition in a core-softened potential system. *Physica A* **2020**, *550*, 124521. [\[CrossRef\]](#)
40. Fomin, Y. A comparison of dynamic properties of a core-softened system of particles across glass transition, melting and random tiling formation. *Phys. Chem. Liq.* **2019**, *58*, 290–301. [\[CrossRef\]](#)
41. Dubinin, N.; Filippov, V.; Vatolin, N. Structure and thermodynamics of the one- and two-component square-well fluid. *J. Non-Cryst. Solids* **2007**, *353*, 1798–1801. [\[CrossRef\]](#)
42. Ornstein, L.S.; Zernice, F. Interference of rontgen rays. *Proc. Acad. Sci.* **1914**, *17*, 793.
43. Lebowitz, J.L.; Percus, J.K. Mean Spherical Model for Lattice Gases with Extended Hard Cores and Continuum Fluids. *Phys. Rev.* **1966**, *144*, 251–258. [\[CrossRef\]](#)
44. Helfand, E. Theory of the Molecular Friction Constant. *Phys. Fluids* **1961**, *4*, 681–691. [\[CrossRef\]](#)
45. Davis, H.T. Contribution to the Friction Coefficient from Time Correlations between Hard and Soft Molecular Interactions. *J. Chem. Phys.* **1967**, *46*, 4043–4047. [\[CrossRef\]](#)

46. Dubinin, N.E. Self-diffusion coefficients of liquid alkali metals described by the square-well model within the mean spherical approximation. *Indian J. Pure Appl. Phys.* **2015**, *53*, 392–394.
47. Dubinin, N.E. The SW-MSA Calculation of Self-Diffusion Coefficients in Liquid Lithium and Rubidium. *Acta Phys. Pol. A* **2016**, *129*, 310–312. [\[CrossRef\]](#)
48. Dubinin, N.E. Square-well self-diffusion coefficients in liquid binary alloys of alkali metals within the mean spherical approximation. *J. Alloys Compd.* **2019**, *803*, 1100–1104. [\[CrossRef\]](#)
49. Einstein, A. Über die von der molekularkinetischen Theorie der Wärme geforderte Bewegung von in ruhenden Flüssigkeiten suspendierten Teilchen. *Ann. Phys.* **1905**, *322*, 549–560. (In German) [\[CrossRef\]](#)
50. Croxton, C.A. *Liquid State Physics—A Statistical Mechanical Introduction*; Cambridge University Press: Cambridge, UK, 1974.
51. Iida, T.; Guthrie, R.I.L. *The Physical Properties of Liquid Metals*; Clarendon Press: Oxford, UK, 1988.
52. Longuet-Higgins, H.; Valleau, J. Transport coefficients of dense fluids of molecules interacting according to a square well potential. *Mol. Phys.* **1958**, *1*, 284–294. [\[CrossRef\]](#)
53. Wertheim, M.S. Exact Solution of the Percus-Yevick Integral Equation for Hard Spheres. *Phys. Rev. Lett.* **1963**, *10*, 321–323. [\[CrossRef\]](#)
54. Thiele, E. Equation of State for Hard Spheres. *J. Chem. Phys.* **1963**, *39*, 474–479. [\[CrossRef\]](#)
55. Waseda, Y. *The Structure of Non-Crystalline Materials*; McGraw-Hill: New York, NY, USA, 1980.
56. Henderson, J.; Yang, L. Self-diffusion of copper in molten copper. *Trans. Met. Soc. AIME* **1961**, *221*, 72.
57. Mitrokhin, Y. Comparison of simulations of liquid metals by classical and ab initio molecular dynamics. *Comput. Mater. Sci.* **2006**, *36*, 189–193. [\[CrossRef\]](#)
58. Liu, D.; Qin, J.; Gu, T. The structure of liquid Mg–Cu binary alloys. *J. Non-Cryst. Solids* **2010**, *356*, 1587–1592. [\[CrossRef\]](#)
59. Alemany, M.M.G.; Rey, C.; Gallego, L.J. Transport coefficients of liquid transition metals: A computer simulation study using the embedded atom model. *J. Chem. Phys.* **1998**, *109*, 5175–5176. [\[CrossRef\]](#)
60. Chen, F.; Zhang, H.F.; Qin, F.X.; Hu, Z.Q. Molecular dynamics study of atomic transport properties in rapidly cooling liquid copper. *J. Chem. Phys.* **2004**, *120*, 1826–1831. [\[CrossRef\]](#)
61. Han, X.; Chen, M.; Lu, Y.J. Transport Properties of Undercooled Liquid Copper: A Molecular Dynamics Study. *Int. J. Thermophys.* **2008**, *29*, 1408–1421. [\[CrossRef\]](#)
62. Mei, J.; Davenport, J.W. Molecular-dynamics study of self-diffusion in liquid transition metals. *Phys. Rev. B* **1990**, *42*, 9682–9684. [\[CrossRef\]](#)
63. Cheng, H.; Lü, Y.J.; Chen, M. Interdiffusion in liquid Al–Cu and Ni–Cu alloys. *J. Chem. Phys.* **2009**, *131*, 044502. [\[CrossRef\]](#)
64. Qi, Y.; Wang, L.; Fang, T. Demixing behaviour in binary Cu–Co melt. *Phys. Chem. Liq.* **2013**, *51*, 687–694. [\[CrossRef\]](#)
65. Leak, V.G.; Swalin, R.A. *Trans. Met. Soc. AIME* **1964**, *230*, 426. Available online: https://scholar.google.com/scholar_lookup?title=&journal=Trans.%20TMS-AIME&volume=230&pages=426-30&publication_year=1964&author=Leak%20V.G.&author=Swalin%20R.A (accessed on 8 October 2020).
66. Pasturel, A.; Tasci, E.S.; Sluiter, M.H.F.; Jakse, N. Structural and dynamic evolution in liquid Au–Si eutectic alloy by ab initio molecular dynamics. *Phys. Rev. B* **2010**, *81*, 40202. [\[CrossRef\]](#)
67. Peng, H.-L.; Voigtmann, T.; Kolland, G.; Kobatake, H.; Brillo, J. Structural and dynamical properties of liquid Al–Au alloys. *Phys. Rev. B* **2015**, *92*, 184201. [\[CrossRef\]](#)
68. Bogicevic, A.; Hansen, L.B.; Lundqvist, B.I. Simulations of atomic structure, dynamics, and self-diffusion in liquid Au. *Phys. Rev. E* **1997**, *55*, 5535–5545. [\[CrossRef\]](#)

Publisher’s Note: MDPI stays neutral with regard to jurisdictional claims in published maps and institutional affiliations.



© 2020 by the author. Licensee MDPI, Basel, Switzerland. This article is an open access article distributed under the terms and conditions of the Creative Commons Attribution (CC BY) license (<http://creativecommons.org/licenses/by/4.0/>).